Cellular/Molecular

Amplified Mechanically Gated Currents in Distinct Subsets of Myelinated Sensory Neurons following *In Vivo* Inflammation of Skin and Muscle

Andy D. Weyer, Crystal L. O'Hara, and Cheryl L. Stucky
Department of Cell Biology, Neurobiology, and Anatomy, Medical College of Wisconsin, Milwaukee, Wisconsin 53226

Primary afferents are sensitized to mechanical stimuli following *in vivo* inflammation, but whether sensitization of mechanically gated ion channels contributes to this phenomenon is unknown. Here we identified two populations of murine A fiber-type sensory neurons that display markedly different responses to focal mechanical stimuli of the membrane based on their expression of calcitonin gene-related peptide (CGRP). Following inflammation of the hindpaw, myelinated, CGRP-positive neurons projecting to the paw skin displayed elevated mechanical currents in response to mechanical stimuli. Conversely, muscle inflammation markedly amplified mechanical currents in myelinated, CGRP-negative neurons projecting to muscle. These data show, for the first time, that mechanically gated currents are amplified following *in vivo* tissue inflammation, and also suggest that mechanical sensitization can occur in myelinated neurons after inflammation.

Key words: **Aβ; Aδ; mechanosensation; mechanotransduction; pain; sensitization**

Introduction

Following peripheral injury, behavioral sensitization to mechanical stimuli is well established, and experiments have demonstrated that at least part of this sensitization is due to increased firing rates of peripheral nociceptive nerve fibers (Andrew and Greenspan, 1999; Lennertz et al., 2012). Yet, beyond a few *in vitro* studies in which inflammatory modulators are applied directly to neuronal cell bodies (Di Castro et al., 2006; Dubin et al., 2012; Kubo et al., 2012; Eijkelkamp et al., 2013), no reports have yet examined whether mechanically gated currents themselves are sensitized following bona fide *in vivo* inflammation.

In addition to mechanotransduction on the molecular level, another area of increasing discussion is the role of myelinated afferents in pain sensation. Traditionally, pain is thought to be carried largely by unmyelinated C fibers (ongoing pain) and some lightly myelinated Aδ fibers (sharp initial pain). However, increasing evidence has argued for a larger role for myelinated afferents in mediating pain sensation. For instance, some Aβ fibers may serve as nociceptors under basal conditions (Djouhri and Lawson, 2004; Woodbury et al., 2008). During neuropathic pain, both low-threshold Aβ and high threshold Aδ mechanoreceptors (both of which are myelinated) exhibit increased firing rates or reduced firing thresholds to sustained mechanical stimuli (Campbell et al., 1988; Smith et al., 2013; Boada et al., 2014). Additionally, some evidence suggests that Aβ afferents may release nociceptive peptides, such as calcitonin gene-related peptide (CGRP), and may also form novel connections with nociceptive projection neurons in lamina I and II of the dorsal horn after peripheral inflammation (Woolf et al., 1992; Neumann et al., 1996; Baba et al., 1999). Thus, the contribution of myelinated afferents to pain after peripheral injury is far from defined.

Taking these deficiencies in somatosensory knowledge into account, we sought to determine what effect *in vivo* injury has on mechanically gated currents in putatively myelinated neurons. Here we show that specific subclasses of myelinated neurons display elevated currents in response to mechanical stimuli following inflammation and that this amplification is dependent upon whether the inflammation occurs in cutaneous or muscular tissue.

Materials and Methods

Animals. Heterozygous male mice (6–24 weeks old, randomly assigned to groups) expressing GFP under the CGRPα (*calca*) promoter (McCoy et al., 2012) were used in all patch-clamp experiments for visualization of peptidergic neuronal populations. Mice had *ad libitum* access to food and water and were housed on a 14:10 h light/dark cycle. All animal protocols were approved by the Institutional Animal Care and Use Committee of the Medical College of Wisconsin.

Retrograde tracer injections. To label sensory neurons projecting to either skin or muscle, we injected the retrograde tracer Wheat Germ Agglutinin-AF594 (WGA, 1% in PBS, Invitrogen) into either the saphenous nerve (innervates the dorsal hindpaw) or the gastrocnemius muscle.

Received Feb. 9, 2015; revised May 11, 2015; accepted May 20, 2015.

Author contributions: A.D.W. and C.L.S. designed research; A.D.W. and C.L.O. performed research; A.D.W. and C.L.S. analyzed data; A.D.W. and C.L.S. wrote the paper.

This work was supported by National Institutes of Health Grants NS040538 and NS070711 to C.L.S. We thank Katherine J. Zappia and Francie Möhring for their critical review of the manuscript.

The authors declare no competing financial interests.

Correspondence should be addressed to Dr. Cheryl L. Stucky, Medical College of Wisconsin, 8701 Watertown Plank Road, BSB 428, Milwaukee, WI 53226. E-mail: cstucky@mcw.edu.

DOI:10.1523/JNEUROSCI.0549-15.2015

 0270-6474/15/359456-07$15.00/0

Saphenous nerve injections were performed as previously described (Malin et al., 2011). Briefly, the nerve was cut away from the surrounding connective tissue, a piece of Parafilm placed underneath it to prevent tracer leakage, and ~5 μl of WGA injected subepineurally with a borosilicate pipette. Muscle injections were performed by injecting 20 μl of tracer into the gastrocnemius muscle through a 29-gauge needle in multiple spots.

Retrograde transport from the injection target to the DRG required 5 d, so animals were killed for DRG isolation and culturing on the fifth day after injection.

Pain induction. For cutaneous inflammation, mice were injected subcutaneously with 30 μl of complete Freud's adjuvant (CFA) into the plantar aspect of the hindpaw on the third day following WGA injection. Mice were then killed 2 d after CFA injection, corresponding with the time point of greatest sensitivity (Lennertz et al., 2012). For muscle inflammation, mice were injected in two locations with 30 μl of CFA (60 μl total) on the third day following WGA injection. Mice were then killed 2 d after CFA injection.

Acid injections were performed as previously described (Sluka et al., 2001): mice were injected with 100 μl of pH 4.0 saline on the first and third days following WGA injection. Mice were then killed 2 d after the last acid injection.

Sensory neuron isolation and culturing. To obtain sensory neurons, mice were decapitated and lumbar DRGs 2–5 were removed and incubated in solutions containing 10 mg/ml collagenase for 40 min and 0.5% trypsin for 45 min. DRGs were then mechanically dissociated and plated onto laminin-coated glass coverslips, followed by overnight incubation in media containing DMEM and Hams F12, supplemented with 10% heat-inactivated horse serum, 2 mM L-glutamine, 0.41% D-glucose, 100 units penicillin, and 100 μg/ml streptomycin.

Electrophysiology. Following overnight culture, isolated sensory neurons were used for patch-clamp experiments. Coverslips were placed in a recording chamber situated over an inverted microscope and were continuously superfused with an extracellular buffer consisting of the following: 140 mM NaCl, 5 mM KCl, 2 mM $CaCl_2$, 1 mM $MgCl_2$, 10 mM HEPES, and 10 mM glucose, pH 7.4 ± 0.03 and 310 ± 3 mOsm.

Neurons were patched using borosilicate pipettes with resistances of 2.4–5 MΩ and were filled with a solution containing 135 mM KCl, 10 mM NaCl, 1 mM $MgCl_2$, 1 mM EGTA, 0.2 mM NaGTP, 2.5 mM $ATPNa_2$, and 10 mM HEPES, pH 7.20 ± 0.03 and 290 ± 3 mOsm.

Neuronal capacitance was compensated for, and series resistance was kept <10 MΩ and compensated at 60%. Action potentials were elicited via stepwise square pulse current injections in current-clamp mode to obtain rheobase values.

Mechanically gated currents were elicited in voltage-clamp mode by indenting the soma membrane with a glass pipette (tip diameter ~1–2 μm) driven by a piezo stack actuator (PA25, PiezoSystem) moving at ~106.25 μm/ms. The pipette tip was advanced in increasing displacements of 1.82 μm held for 200 ms, with 25 s given between steps to avoid sensitization/desensitization of currents. Recordings were made using an EPC9 amplifier (HEKA Electronics) and Pulse software (HEKA Electronics).

Immunofluorescence. The anti-neurofilament 200 antibody (N52 clone, Sigma) was used at a concentration of 1:20,000, and the anti-parvalbumin antibody (Abcam) was used at a concentration of 1:10,000. An anti-rabbit secondary conjugated to AlexaFluor-488 (Invitrogen) was used at a concentration of 1:500.

Data analysis/statistics. Only neurons for which the leak current was ≤300 pA were analyzed. Recordings for which the patch seal could not be maintained for at least 3.6 μm of membrane indentation were discarded. Patch-clamp data were analyzed using Pulse, PulseFit, or Fitmaster software (HEKA Electronics). The time constants of inactivation (τ) obtained from the decay kinetics were used to categorize neurons as rapidly inactivating (RI, $\tau < 10$ ms), intermediately inactivating (10 ms ≤ τ ≤ 30 ms), or slowly inactivating ($\tau > 30$ ms). Neurons classified as mechanically insensitive did not respond to focal probing with a current amplitude > 20 pA to any stimulation.

The statistical test used for each figure is noted in the figure legend, and all graphs show mean ± SEM unless noted otherwise.

Results

CGRP expression delineates functional subgroups of large-diameter neurons

We first sought to subtype large-diameter sensory neurons (diameter > 27 μm; mean, 34.05; range, 27.2–48), which correspond to myelinated Aβ and Aδ afferents *in vivo* (Dirajlal et al., 2003). We therefore used a mouse line in which GFP is expressed under the CGRPα (*calca*) promoter (McCoy et al., 2012), allowing us to visually categorize sensory neurons as CGRP-positive or -negative (Fig. 1*A*). Previous characterization of this mouse line demonstrated strong fidelity between GFP expression and CGRP immunoreactivity (McCoy et al., 2012). Additionally, we further subtyped large-diameter neurons based on their innervation target by injecting the retrograde tracer WGA-AF594 into either the saphenous nerve (subepineural injection) or the gastrocnemius muscle (intramuscular injection) (Fig. 1*A*). Traditionally, CGRP is associated with the peptidergic subset of small-diameter, C fiber-type sensory neurons. However, we found that ~50% of all large-diameter neurons were CGRP-positive based on GFP expression (Fig. 1*B*), in accord with recent findings (McCoy and Zylka, 2014).

Patch-clamp studies of these neurons revealed distinct differences between large CGRP-positive and CGRP-negative neurons. CGRP-positive neurons projecting to both skin and muscle displayed significantly lower rheobases (Fig. 1*C*) and wider action potentials (Fig. 1*D*) compared with their CGRP-negative counterparts. In response to focal mechanical probing of the cell soma (Fig. 1*E*), CGRP-negative neurons displayed significantly larger currents over a series of six increasing mechanical steps, regardless of their innervation target (Figs. 1*F*, *G*).

Mechanically gated currents were also categorized as rapidly inactivating (RI), intermediately inactivating, slowly inactivating, or mechanically insensitive, based on their decay kinetics (see Materials and Methods), as previously described (Coste et al., 2010; Hao and Delmas, 2010). For skin-projecting neurons, a greater percentage of CGRP-negative neurons responded to mechanical stimulation with RI currents compared with CGRP-positive neurons (Fig. 1*H*; 96.8% vs 66.7%), and large-diameter CGRP-positive neurons displayed a strong trend for decreased overall responsiveness to mechanical stimuli compared with CGRP-negative neurons (Fig. 1*H*; $p = 0.053$ for mechanically insensitive subtype). However, these proportions were not different between CGRP-positive and -negative neurons projecting to muscle (Fig. 1*H*).

Given these differences in excitability, action potential characteristics, and mechanical responsiveness, we conclude that large-diameter CGRP-positive and CGRP-negative neurons encompass two distinct functional classes of putatively myelinated sensory neurons.

Large-diameter CGRP-positive and -negative somata are predominantly myelinated

Because CGRP has been traditionally correlated with C fiber-type neurons, we next wanted to determine whether these large-diameter, CGRP-positive neurons were actually myelinated. We therefore stained neurons using the N52 clone of anti-Neurofilament 200, a widely used marker of myelination (Fig. 2*A*, top and middle panels). As expected, almost all (82%–100%) large-diameter neurons (>27 μm) from skin or muscle stained positively for N52, regardless of whether they expressed CGRP (Fig. 2*B*).

Whereas cutaneous myelinated afferents innervate a wide variety of end organs *in vivo*, many myelinated muscle-projecting

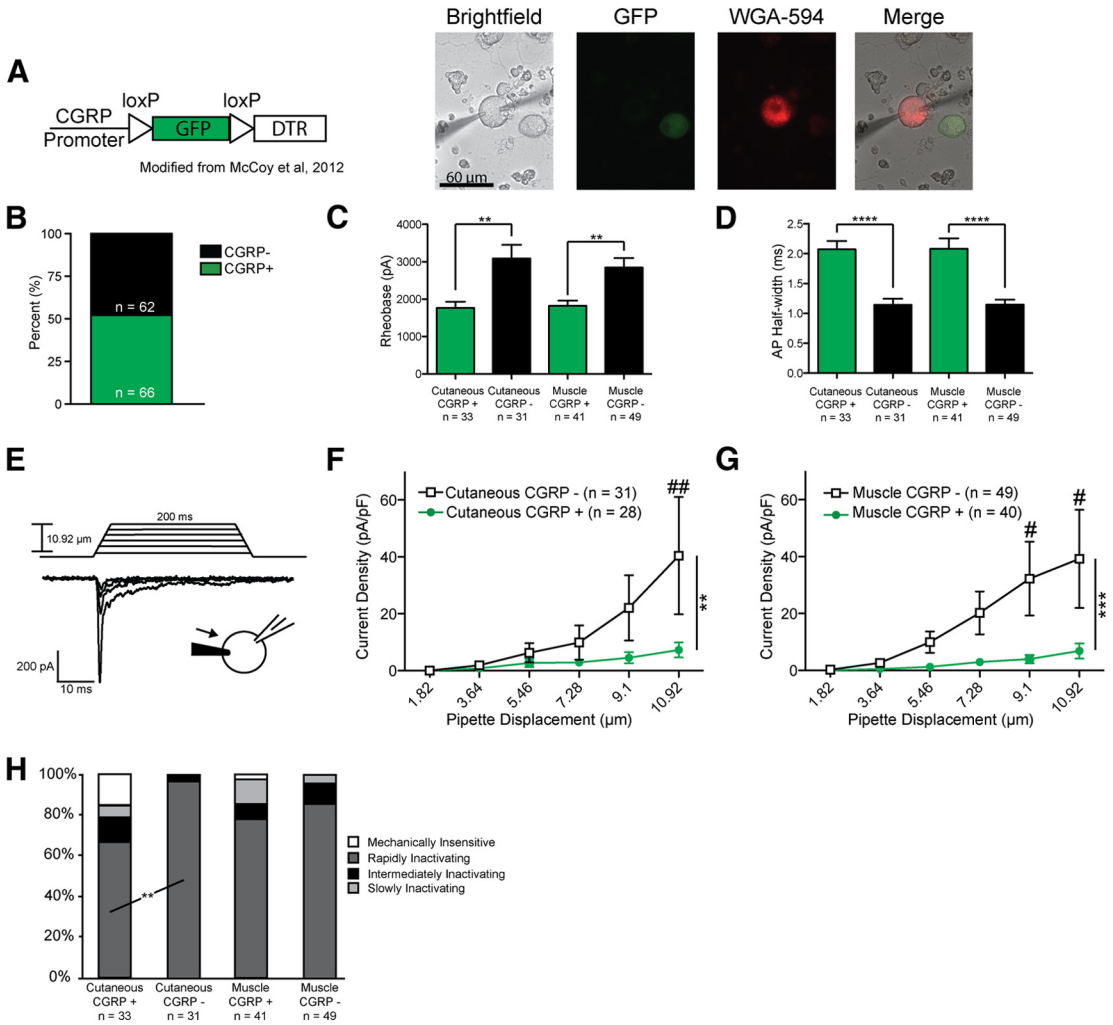

Figure 1. Large-diameter CGRP-positive and -negative neurons represent two distinct classes of sensory neurons. ***A***, Left, Schematic indicating insertion of a GFP-encoding sequence under the direction of the CGRPα (*calca*) promoter. Right, Cultured sensory neurons from a CGRP-GFP mouse injected with the retrograde tracer WGA. ***B***, Approximately half of large-diameter neurons (diameter $>$ 27 μm) expressed CGRP. ***C***, CGRP-positive neurons exhibit lower rheobases compared with CGRP-negative neurons. $^{**}p = 0.0014$ for cutaneous and 0.0011 for muscle (Student's *t* test, df = 60 and 86, respectively). ***D***, Action potentials are wider in large-diameter CGRP-positive neurons. $^{****}p < 0.0001$ (Student's *t* test, df = 60 and 86, respectively). ***E***, Example traces demonstrating increased current magnitude in response to mechanical stimulation of the soma with increasing pipette displacements. ***F***, ***G***, Mechanically gated currents elicited from large-diameter CGRP-negative neurons are much larger over a series of six increasing indentations compared with CGRP-positive neurons for both skin-projecting (***F***) and muscle-projecting (***G***) neurons. Data are presented as current density (pA/pF). ***F***, $^{**}p < 0.0017$ (two-way ANOVA; Bonferroni *post hoc* analysis used for multiple comparisons). ***G***, $^{***}p = 0.0002$ (two-way ANOVA; Bonferroni *post hoc* analysis used for multiple comparisons). $^{\#\#}p = 0.0016$, $^{\#}p = 0.0249$ at 9.1 μm and $p = 0.0165$ at 10.92 μm. ***H***, Mechanical stimulation elicited a significantly higher number of currents with rapidly inactivating kinetics in large-diameter CGRP-negative neurons projecting to skin compared with CGRP-positive neurons projecting to skin. $^{**}p = 0.0028$ (Fisher's exact test). No difference in current kinetics was observed in response to mechanical stimulation in muscle-projecting large-diameter neurons.

afferents are thought to innervate muscle spindles for proprioception. To verify this assertion, we stained cultured neurons with an antibody directed against parvalbumin, a marker of proprioceptive neurons (Celio, 1990) (Fig. 2*A*, bottom panel). Interestingly, only 10% of muscle-projecting, myelinated CGRP-negative neurons and no CGRP-positive neurons stained positively for parvalbumin (Fig. 2*C*). This indicates that the vast majority of the myelinated muscle-projecting neurons used in this study are unlikely to be proprioceptors.

Cutaneous inflammation sensitizes CGRP-positive A fiber neurons to mechanical stimuli

Given the conflicting evidence on mechanical sensitization of myelinated afferents following inflammation (Andrew and Greenspan, 1999; Potenzieri et al., 2008; Kubo et al., 2012; Lennertz et al., 2012) and the lack of data demonstrating amplification of mechanically gated currents in any neuronal subtype after inflammation *in vivo*, we next examined whether myelinated CGRP-positive and CGRP-negative neurons display altered functional properties following inflammation of their peripheral targets.

We first created cutaneous inflammation by injecting 30 μl of CFA into the hindpaw of the WGA-injected leg, which induced a significant inflammatory response affecting both the glabrous skin and the hairy skin innervated by the saphenous nerve. Two days later, in accord with the time point of greatest mechanical sensitization, DRGs were removed and cultured (Lennertz et al., 2012). When large CGRP-negative neurons projecting to the inflamed paw were mechanically stimulated, no difference was noted in current densities or current kinetics compared with baseline (Fig. 3*A*,*B*).

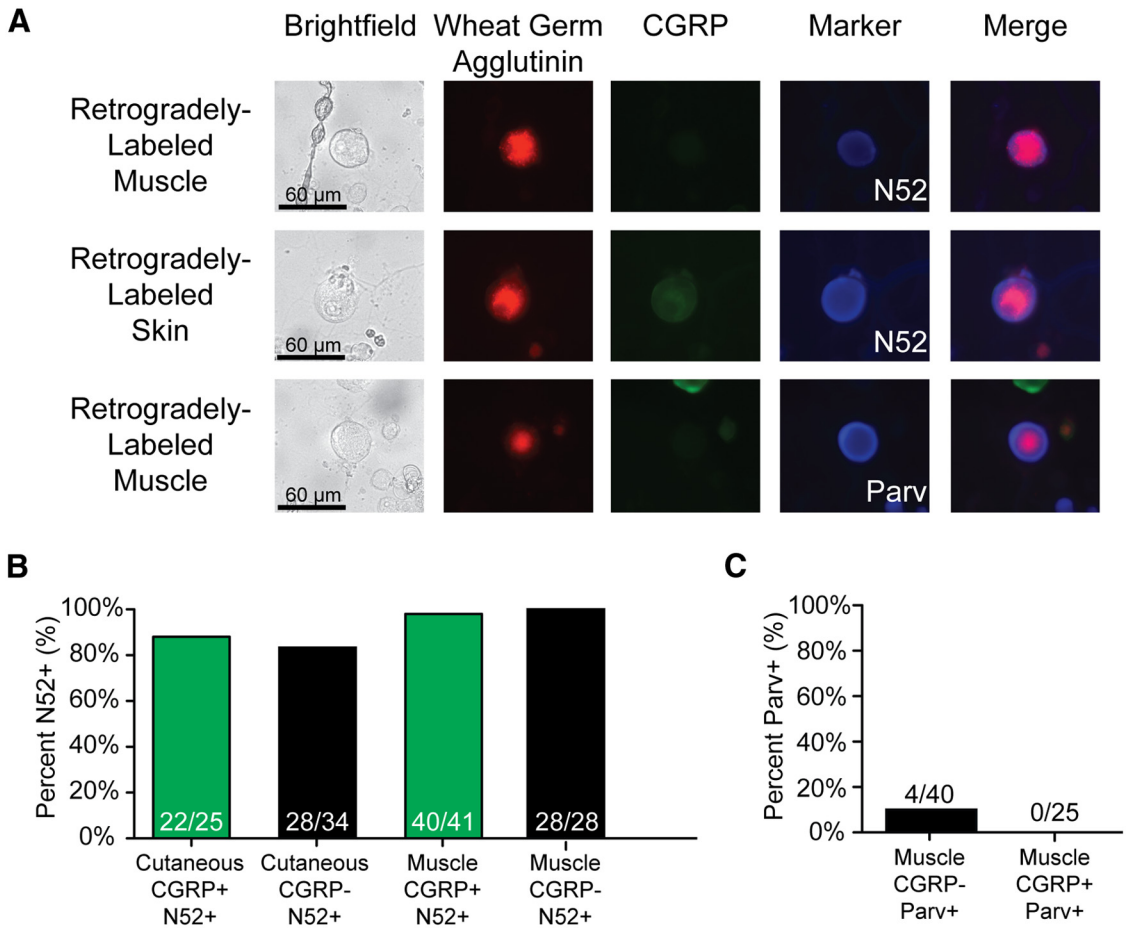

Figure 2. The vast majority of large-diameter neurons are myelinated, and few express the proprioceptive marker parvalbumin. ***A***, Examples of retrogradely labeled large-diameter neurons and their expression of CGRP, N52, or parvalbumin. Top row, Large-diameter CGRP-negative, muscle-projecting, N52-positive neuron. Middle row, Large-diameter CGRP-positive, skin-projecting, N52-positive neuron. Lower row, Large-diameter CGRP-negative, muscle-projecting, parvalbumin-positive neuron. ***B***, A total of 82%–100% of large-diameter neurons are N52-positive. ***C***, Few neurons projecting to muscle are parvalbumin-positive.

In contrast, the large cutaneous CGRP-positive neurons, which displayed small mechanical currents under PBS-injected conditions, exhibited a 4.7-fold elevation in current amplitude following inflammation of the paw (Fig. 3*C*). No changes were noted in current kinetics following inflammation (Fig. 3*D*), but mechanical thresholds were significantly reduced in large CGRP-positive neurons projecting to inflamed skin (Fig. 3*E*).

We also examined the decay kinetics of RI currents following CFA injection because previous research has demonstrated that Piezo2, the major mechanotransducer in myelinated afferents (Ranade et al., 2014), displays delayed inactivation *in vitro* after direct exposure to bradykinin (Dubin et al., 2012). However, the decay kinetics of RI currents (τ) were unaltered by inflammation (Fig. 3*F*), suggesting that the amplification of mechanically gated currents in this study may not be due to actions on Piezo2.

Importantly, these findings could not be explained by *de novo* expression of CGRP, as an examination of the percentage of large-diameter neurons expressing CGRP revealed no differences between the naive state and the inflammatory state (48.8% under naive conditions, 42.5% under CFA conditions) (Fig. 3*G*).

Together, these data strongly suggest that *in vivo* inflammation of skin amplifies mechanically activated currents in putatively myelinated CGRP-expressing afferents.

In muscle, CFA, but not acid, causes sensitization to mechanical stimuli in myelinated CGRP-negative neurons

Given the sensitization of large-diameter, CGRP-positive neurons following cutaneous inflammation, we next asked whether the same phenomenon could be observed in large-diameter neurons innervating injured muscle. We used two different models of muscle pain: the dual-acid injection model (2×100 μl injections of pH 4.0 PBS into the gastrocnemius) (Sluka et al., 2001), and a 60 μl injection of CFA into the gastrocnemius muscle.

In stark contrast to the effects observed with cutaneous inflammation, CGRP-positive neurons projecting to CFA- or acid-injected muscle displayed no sensitization to mechanical stimuli compared with baseline (Fig. 4*A*,*B*); indeed, large CGRP-positive neurons from the acid group actually exhibited a slight reduction in current densities (Fig. 4*A*). Additionally, no difference was observed in the distribution of current kinetics following CFA or acid injection (Fig. 4*C*).

Similarly, CGRP-negative neurons projecting to muscle also exhibited no difference in current amplitude or kinetics upon acid injection (Fig. 4*D*,*F*). However, CFA injections into the gastrocnemius muscle caused an almost threefold amplification of mechanical currents in large-diameter, CGRP-negative neurons (Fig. 4*E*), and also resulted in reduced mechanical thresholds (Fig. 4*H*). This amplification was not

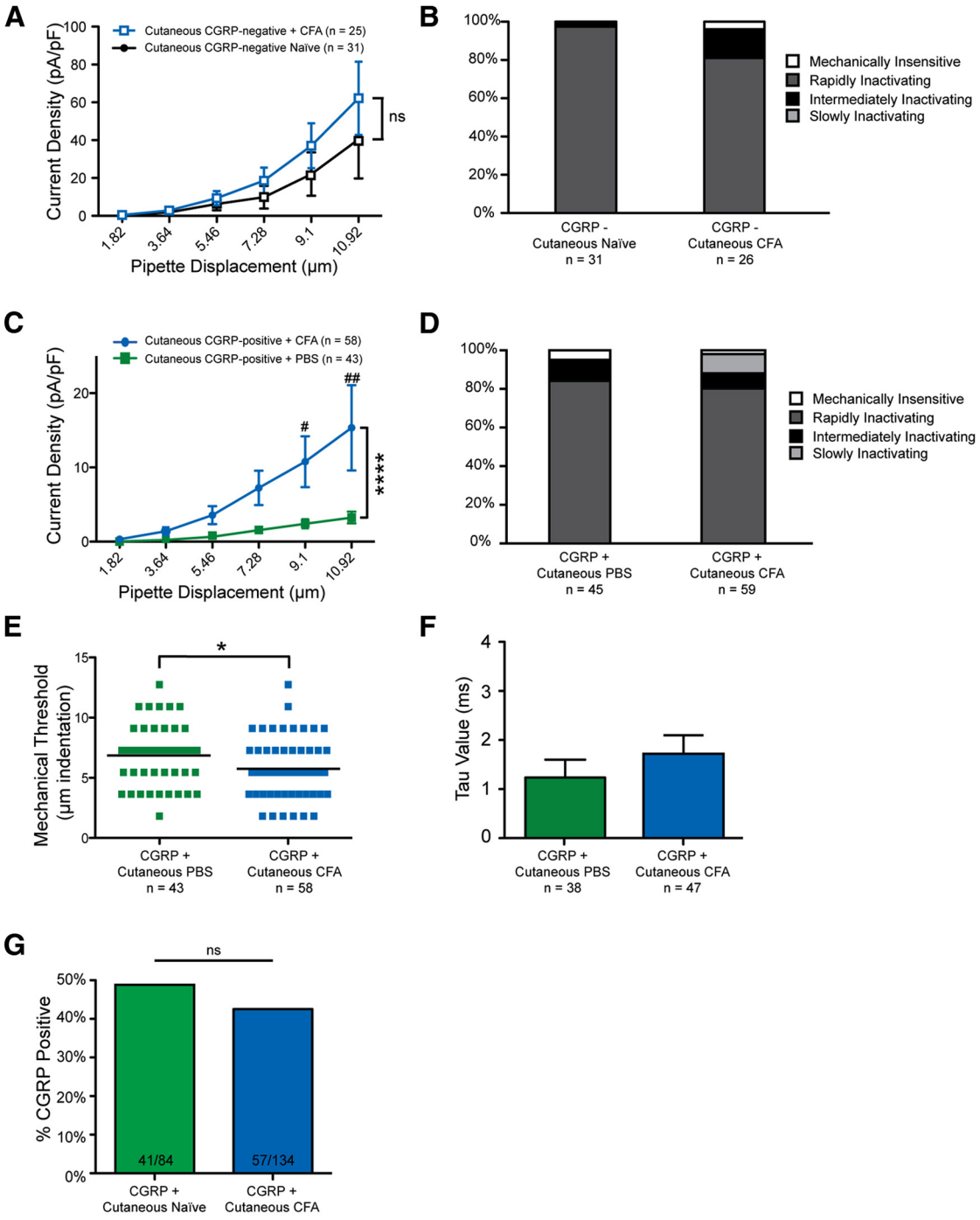

Figure 3. Myelinated CGRP-positive neurons exhibit larger mechanical currents following cutaneous inflammation. ***A***, Skin-projecting, myelinated CGRP-negative neurons display similar current amplitudes under both naive conditions and after CFA-mediated inflammation ($p = 0.0705$, two-way ANOVA, df = 1). ns, Not significant. ***B***, Current kinetics are unchanged in A fiber-type CGRP-negative neurons following cutaneous inflammation ($p = 0.1367$, χ^2 test, df = 2). ***C***, Skin-projecting, myelinated CGRP-positive neurons exhibit larger current amplitudes following cutaneous inflammation. $^{****}p < 0.0001$ (two-way ANOVA, df = 1). $^{\#\#}p = 0.0021$ (Bonferroni *post hoc*). $^{\#}p = 0.0305$ (Bonferroni *post hoc*). ***D***, Current kinetics are unchanged in large CGRP-positive neurons following cutaneous inflammation ($p = 0.1386$, χ^2 test, df = 2). ***E***, Mechanical thresholds were reduced in myelinated CGRP-positive neurons following inflammation. $^{*}p = 0.0359$ (Mann–Whitney test). ***F***, The τ of RI currents was unchanged in myelinated CGRP-positive neurons following cutaneous inflammation ($p = 0.3599$, Student's *t* test). ***G***, The proportion of skin-projecting, CGRP-positive large neurons was unchanged following inflammation ($p = 0.4026$, Fisher's exact test).

accompanied by changes in current kinetics (Fig. 4*F*), and no changes in the time constant of inactivation of RI currents were observed following either acid or CFA injections (Fig. 4*G*), suggesting that the current amplification may not be attributable to Piezo2.

Collectively, these data indicate that myelinated neurons projecting to muscle can also be sensitized to mechanical stimuli, but that this sensitization occurs in A fiber-type neurons that do not express CGRP and is dependent on the mode of muscle injury.

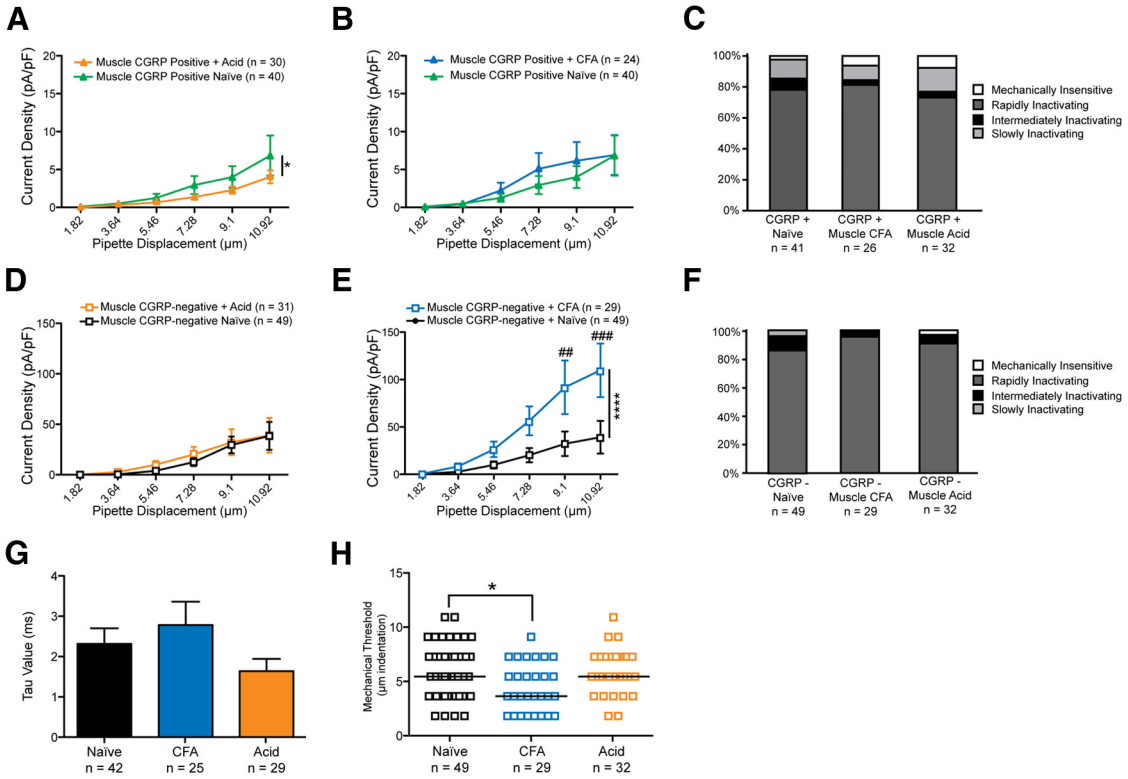

Figure 4. Large-diameter CGRP-negative neurons projecting to muscle exhibit larger mechanically gated currents following muscle inflammation. ***A***, Myelinated CGRP-positive neurons exhibit a small, but significant, reduction in mechanically gated current amplitudes following acid injection of muscle. $^{*}p = 0.0392$ (two-way ANOVA, df = 1). ***B***, Myelinated CGRP-positive neurons exhibit no change in current amplitudes following CFA-mediated muscle inflammation ($p = 0.2856$, two-way ANOVA, df = 1). ***C***, No changes in current kinetics were observed in large-diameter CGRP-positive neurons following acid- or CFA-induced muscle injury ($p = 0.8920$, χ^2 test). ***D***, Myelinated CGRP-negative neurons display unaltered current amplitudes following acid-mediated muscle injury ($p = 0.4946$, two-way ANOVA). ***E***, Myelinated CGRP-negative neurons display a threefold amplification of mechanically gated current magnitude following CFA-mediated muscle inflammation. $^{****}p < 0.0001$ overall (two-way ANOVA). $^{\#\#}p = 0.0029$ (Bonferroni test for multiple comparisons). $^{\#\#\#}p = 0.0009$ (Bonferroni test for multiple comparisons). ***F***, Current kinetics in large-diameter CGRP-negative neurons were unaltered by either CFA- or acid-mediated muscle injury ($p = 0.4406$, χ^2 test, df = 6). ***G***, The τ for RI currents was unchanged by CFA- or acid-mediated muscle injury compared with naive controls ($p = 0.2172$, one-way ANOVA, df = 2). ***H***, Mechanical thresholds were significantly reduced in myelinated CGRP-negative neurons projecting to muscle following CFA-mediated injury ($p = 0.0364$, Kruskal–Wallis test). $^{*}p = 0.0365$ (Bonferroni test for multiple comparisons).

Discussion

Here we have shown that myelinated neurons have distinct mechanosensitive phenotypes based on their expression of CGRP and, for the first time, that mechanically gated currents are amplified following an inflammatory insult *in vivo*. Specifically, our data indicate that mechanically gated currents are elevated in myelinated CGRP-positive neurons following cutaneous inflammation, and, conversely, in myelinated CGRP-negative neurons following muscle inflammation. Critically, these data suggest that mechanically gated currents themselves may be amplified as a result of inflammatory processes and that sensitization to mechanical stimuli following injury is not just the result of changes in voltage-gated ion channel gating or expression.

The role of myelinated fibers following peripheral inflammation

In addition to these findings, other research has increasingly implicated myelinated cutaneous fibers for their roles in ongoing inflammatory pain. Injection of algesic agents, such as formalin, cause a robust nociceptive response in rodents that involves input from both Aβ- and Aδ-myelinated afferents (Puig and Sorkin, 1996), and Aβ fibers may release nociceptive compounds, such as substance P, onto dorsal horn neurons following peripheral inflammation (Neumann et al., 1996). Additional research has gone further and demonstrated that firing rates of Aδ fibers are sensitized in response to mechanical stimuli following cutaneous inflammation (Meyer et al., 1991; Andrew and Greenspan, 1999; Potenzieri et al., 2008), although studies from our own laboratory could not confirm this (Lennertz et al., 2012).

In muscle, we observed mechanical sensitization in CGRP-negative neurons, but only in response to CFA injections, and not acid injections. The dual acid injection model (Sluka et al., 2001) is widely used by researchers examining muscle pain, but current evidence suggests that installation of this pain is mediated by acid-sensing ion channels on C fiber-type neurons (Walder et al., 2010), and that maintenance of this hyperalgesia is centrally mediated (Gautam et al., 2012). This correlates well with the lack of mechanical sensitization in either CGRP-positive or CGRP-negative myelinated neurons following acid-mediated injury.

The large CGRP-negative neurons examined here may correspond to Group III afferents *in vivo*, as they are also lightly myelinated, highly sensitive to stretch, and have narrow action potentials (Abrahams, 1986; Jankowski et al., 2013). Because Group III afferents contribute to pain sensation (Rotto and Kaufman, 1988), it is perhaps unsurprising that large CGRP-negative neurons exhibited amplified currents after muscle inflammation.

Despite an inability to differentiate between Aβ and Aδ fiber-type neurons in this study, our findings add to the evidence supporting a role for myelinated fibers in inflammatory pain, and go further by demonstrating that the sensitization is due at least in

part to effects on the initial mechanotransduction machinery at the sensory neuron membrane.

Potential mechanisms for mechanically gated current sensitization

The key question remaining, then, is what process mediates mechanical sensitization after inflammation of muscle or skin. Multiple possibilities exist, including increased expression of genes involved in mechanosensation, increased trafficking of mechanosensitive proteins to the plasma membrane, or post-translational modifications of mechanosensitive proteins. Future research will be required to explore these possibilities.

Regardless, these data answer a long unresolved question in the field: whether mechanically gated currents play a role in the sensitization to mechanical stimuli during peripheral inflammation. Our data strongly suggest that the widely reported sensitization to mechanical stimuli following injury on the behavioral and afferent levels is due at least in part to an amplification of mechanically gated currents at the transduction site. Importantly, these changes can occur in myelinated sensory neurons, which are not normally associated with the inflammatory response, and future research must determine whether targeting myelinated afferents represents a viable treatment for clinical pain conditions.

References

Abrahams VC (1986) Group III and IV receptors of skeletal muscle. Can J Physiol Pharmacol 64:509–514. CrossRef Medline

Andrew D, Greenspan JD (1999) Mechanical and heat sensitization of cutaneous nociceptors after peripheral inflammation in the rat. J Neurophysiol 82:2649–2656. Medline

Baba H, Doubell TP, Woolf CJ (1999) Peripheral inflammation facilitates A_{NL} fiber-mediated synaptic input to the substantia gelatinosa of the adult rat spinal cord. J Neurosci 19:859–867. Medline

Boada MD, Martin TJ, Peters CM, Hayashida K, Harris MH, Houle TT, Boyden ES, Eisenach JC, Ririe DG (2014) Fast-conducting mechanoreceptors contribute to withdrawal behavior in normal and nerve injured rats. Pain 155:2646–2655. CrossRef Medline

Campbell JN, Raja SN, Meyer RA, Mackinnon SE (1988) Myelinated afferents signal the hyperalgesia associated with nerve injury. Pain 32:89–94. CrossRef Medline

Celio MR (1990) Calbindin D-28k and parvalbumin in the rat nervous system. Neuroscience 35:375–475. CrossRef Medline

Coste B, Mathur J, Schmidt M, Earley TJ, Ranade S, Petrus MJ, Dubin AE, Patapoutian A (2010) Piezo1 and Piezo2 are essential components of distinct mechanically activated cation channels. Science 330:55–60. CrossRef Medline

Di Castro A, Drew LJ, Wood JN, Cesare P (2006) Modulation of sensory neuron mechanotransduction by PKC- and nerve growth factor-dependent pathways. Proc Natl Acad Sci U S A 103:4699–4704. CrossRef Medline

Dirajlal S, Pauers LE, Stucky CL (2003) Differential response properties of IB(4)-positive and -negative unmyelinated sensory neurons to protons and capsaicin. J Neurophysiol 89:513–524. CrossRef Medline

Djouhri L, Lawson SN (2004) Aβ-fiber nociceptive primary afferent neurons: a review of incidence and properties in relation to other afferent A-fiber neurons in mammals. Brain Res Rev 46:131–145. CrossRef Medline

Dubin AE, Schmidt M, Mathur J, Petrus MJ, Xiao B, Coste B, Patapoutian A (2012) Inflammatory signals enhance piezo2-mediated mechanosensitive currents. Cell Rep 2:511–517. CrossRef Medline

Eijkelkamp N, Linley JE, Torres JM, Bee L, Dickenson AH, Gringhuis M, Minett MS, Hong GS, Lee E, Oh U, Ishikawa Y, Zwartkuis FJ, Cox JJ, Wood JN (2013) A role for Piezo2 in EPAC1-dependent mechanical allodynia. Nat Commun 4:1682. CrossRef Medline

Gautam M, Benson CJ, Ranier JD, Light AR, Sluka K (2012) ASICs do not play a role in maintaining hyperalgesia induced by repeated intramuscular acid injections. Pain Res Treat 2012:15–18. CrossRef Medline

Hao J, Delmas P (2010) Multiple desensitization mechanisms of mechanotransducer channels shape firing of mechanosensory neurons. J Neurosci 30:13384–13395. CrossRef Medline

Jankowski MP, Rau KK, Ekmann KM, Anderson CE, Koerber HR (2013) Comprehensive phenotyping of group III and IV muscle afferents in mouse. J Neurophysiol 109:2374–2381. CrossRef Medline

Kubo A, Katanosaka K, Mizumura K (2012) Extracellular matrix proteoglycan plays a pivotal role in sensitization by low pH of mechanosensitive currents in nociceptive sensory neurones. J Physiol 590:2995–3007. CrossRef Medline

Lennertz RC, Kossyreva EA, Smith AK, Stucky CL (2012) TRPA1 mediates mechanical sensitization in nociceptors during inflammation. PLoS One 7:e43597. CrossRef Medline

Malin S, Molliver D, Christianson JA, Schwartz ES, Cornuet P, Albers KM, Davis BM (2011) TRPV1 and TRPA1 function and modulation are target tissue dependent. J Neurosci 31:10516–10528. CrossRef Medline

McCoy ES, Zylka MJ (2014) Enhanced behavioral responses to cold stimuli following CGRP α sensory neuron ablation are dependent on TRPM8. Mol Pain 10:1–9. CrossRef Medline

McCoy ES, Taylor-Blake B, Zylka MJ (2012) CGRPα-expressing sensory neurons respond to stimuli that evoke sensations of pain and itch. PLoS One 7:e36355. CrossRef Medline

Meyer RA, Davis KD, Cohen RH, Treede RD, Campbell JN (1991) Mechanically insensitive afferents (MIAs) in cutaneous nerves of monkey. Brain Res 561:252–261. CrossRef Medline

Neumann S, Doubell TP, Leslie T, Woolf CJ (1996) Inflammatory pain hypersensitivity mediated by phenotypic switch in myelinated primary sensory neurons. Nature 384:360–364. CrossRef Medline

Potenzieri C, Brink TS, Pacharinsak C, Simone DA (2008) Cannabinoid modulation of cutaneous Aδ nociceptors during inflammation. J Neurophysiol 100:2794–2806. CrossRef Medline

Puig S, Sorkin LS (1996) Formalin-evoked activity in identified primary afferent fibers: systemic lidocaine suppresses phase-2 activity. Pain 64:345–355. CrossRef Medline

Ranade SS, Woo SH, Dubin AE, Moshourab RA, Wetzel C, Petrus M, Mathur J, Bégay V, Coste B, Mainquist J, Wilson AJ, Francisco AG, Reddy K, Qiu Z, Wood JN, Lewin GR, Patapoutian A (2014) Piezo2 is the major transducer of mechanical forces for touch sensation in mice. Nature 516:121–125. CrossRef Medline

Rotto DM, Kaufman MP (1988) Effect of metabolic products of muscular contraction on discharge of group III and IV afferents. J Appl Physiol 64:2306–2313. Medline

Sluka KA, Kalra A, Moore SA (2001) Unilateral intramuscular injection of acidic saline produce a bilateral, long-lasting hyperalgesia. Muscle Nerve 24:37–46. CrossRef Medline

Smith AK, O'Hara CL, Stucky CL (2013) Mechanical sensitization of cutaneous sensory fibers in the spared nerve injury mouse model. Mol Pain 9:61.

Walder RY, Rasmussen LA, Rainier JD, Light AR, Wemmie JA, Sluka KA (2010) ASIC1 and ASIC3 play different roles in the development of hyperalgesia after inflammatory muscle injury. J Pain 11:210–218. CrossRef Medline

Woodbury CJ, Kullmann FA, McIlwrath SL, Koerber HR (2008) Identity of myelinated cutaneous sensory neurons projecting to nocireceptive laminae following nerve injury in adult mice. J Comp Neurol 508:500–509. CrossRef Medline

Woolf CJ, Shortland P, Coggeshall RE (1992) Peripheral nerve injury triggers central sprouting of myelinated afferents. Nature 355:75–78. CrossRef Medline